



King Saud University  
Arabian Journal of Chemistry

[www.ksu.edu.sa](http://www.ksu.edu.sa)  
[www.sciencedirect.com](http://www.sciencedirect.com)



## ORIGINAL ARTICLE

# Phosphoric acid functionalized graphene oxide: A highly dispersible carbon-based nanocatalyst for the green synthesis of bio-active pyrazoles

Masoumeh Zakeri <sup>a</sup>, Ebrahim Abouzari-lotf <sup>b,c,\*</sup>, Mikio Miyake <sup>a</sup>,  
Shahram Mehdipour-Ataei <sup>d</sup>, Kamyar Shameli <sup>a</sup>

<sup>a</sup> Malaysia–Japan International Institute of Technology, Universiti Teknologi Malaysia, 54100 Kuala Lumpur, Malaysia

<sup>b</sup> Advanced Materials Research Group, Center of Hydrogen Energy, Institute of Future Energy, Universiti Teknologi Malaysia, 54100 Kuala Lumpur, Malaysia

<sup>c</sup> Department of Chemical Engineering, Universiti Teknologi Malaysia, 81310 Johor Bahru, Malaysia

<sup>d</sup> Iran Polymer and Petrochemical Institute, P.O. Box 14965/115, Tehran, Iran

Received 28 September 2017; accepted 9 November 2017

## KEYWORDS

Phosphonated graphene oxide;  
Heterogeneous acidic catalyst;  
Multicomponent reaction;  
Water;  
Pyranopyrazoles;  
Green chemistry

**Abstract** Carbon-based catalysts are gained significant interest for improving a number of catalytic processes due to their unique set of benefits. However, a few of such catalysts are proper for synthesis of organic compounds in water. Therefore, there is a strong need for developing water-tolerant and dispersible catalysts. Here, we demonstrate a simple and efficient method for the preparation of highly dispersible phosphonic acid functionalized carbocatalyst. The applied functionalization method was flexible in controlling the functionalization level. The prepared nanocatalyst exhibited superior catalytic performance toward multicomponent synthesis of pyrano[2,3-*c*]pyrazole, with 80–90% yield within 15 min in water. Moreover, this water-tolerant solid acid catalyst could be simply retrieved and after 6 successive cycles of reactions, the reaction time and yield still keeps within the same level.

© 2017 Production and hosting by Elsevier B.V. on behalf of King Saud University. This is an open access article under the CC BY-NC-ND license (<http://creativecommons.org/licenses/by-nc-nd/4.0/>).

## 1. Introduction

Minimizing environmental risks and designing new eco-safe procedures are becoming an urgent priority in chemistry. On the other hand, it is highly desirable to develop environmentally benign processes that can be conducted in aqueous media (Chanda and Fokin, 2009; Simon and Li, 2012a). Consequently, the design of new, efficient water-based organic reactions with low-cost, step-saving and low-waste production has attracted tremendous research interest in recent years (Ameta

\* Corresponding author at: Advanced Materials Research Group, Center of Hydrogen Energy, Institute of Future Energy, Universiti Teknologi Malaysia, 54100 Kuala Lumpur, Malaysia.

E-mail address: [ebrahim@utm.my](mailto:ebrahim@utm.my) (E. Abouzari-lotf).

Peer review under responsibility of King Saud University.



<https://doi.org/10.1016/j.arabjc.2017.11.006>

1878-5352 © 2017 Production and hosting by Elsevier B.V. on behalf of King Saud University.

This is an open access article under the CC BY-NC-ND license (<http://creativecommons.org/licenses/by-nc-nd/4.0/>).

Please cite this article in press as: Zakeri, M. et al., Phosphoric acid functionalized graphene oxide: A highly dispersible carbon-based nanocatalyst for the green synthesis of bio-active pyrazoles. Arabian Journal of Chemistry (2017), <https://doi.org/10.1016/j.arabjc.2017.11.006>

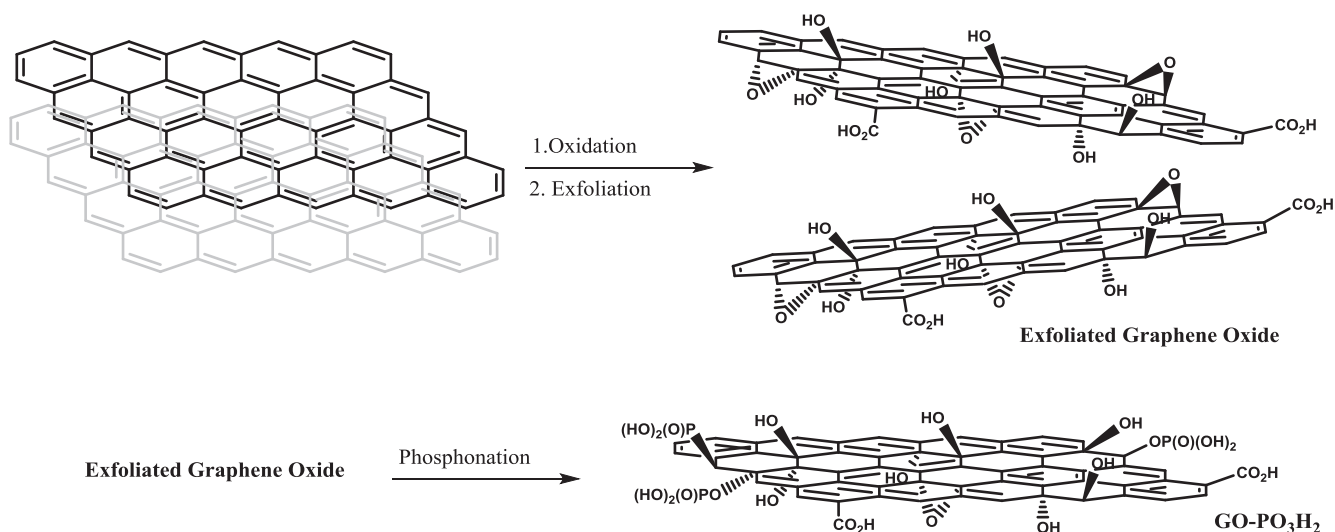


Fig. 1 Synthesis route of phosphonated GO.

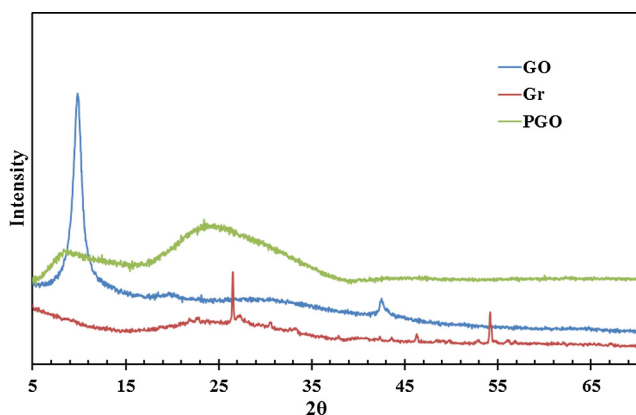


Fig. 2 XRD pattern of graphite, exfoliated GO and phosphonated GO.

and Ameta, 2014; Sangshetti et al., 2017; Simon and Li, 2012b). In addition, there is a strong need for water-tolerant catalysts due to the severe poisoning of the catalytic active sites by water. Typically, most of the solid acids lose their catalytic activities in aqueous media (Okuhara, 2002). In addition, accessibility to the acidic sites is restricted mainly due to the high molecular weight or size and active-site ratios (Cole et al., 2002; Ji et al., 2011). Therefore, there has been a growing interest on the development of new water-tolerant solid acid catalysts with accessible catalytic sites (Chen et al., 2016, 2014; Gromov et al., 2017; Ji et al., 2011; Karimi and Zareyee, 2008; Lin et al., 2015; Liu et al., 2013; Shen et al., 2017).

Nanostructured carbon materials such as activated carbons, (Antonyraj et al., 2014; Jamil et al., 2017; Lv et al., 2015) carbon nanotubes (Hajipour and Khorsandi, 2016; Li et al., 2015), carbon nanofibers (Chinthaginjala et al., 2007; Xie et al., 2016a), and graphene oxides (GO) (Georgakilas et al., 2016) are widely used catalyst supports due to their low cost, superior high surface area and excellent stability (Gupta and Paul, 2014; Su et al., 2013). Particularly, GO has become one of the most widely used catalyst supports due to

its thermodynamic stability, large surface area of up to 2630 m<sup>2</sup> g<sup>-1</sup> and high density of oxygen containing functional groups (Al-Marri et al., 2016). The presence of hydroxyl, carbonyl, epoxide and carboxylic acid groups make GO as a fascinating support to provide covalent attachment of various functional groups while its highly hydrophilic nature stabilizes the dispersion (Garg et al., 2014; Ji et al., 2011; Liu et al., 2016; Navalon et al., 2014; Sengupta et al., 2014; Sun et al., 2013; Tang et al., 2016). In the majority of reports, graphene derivatives have been used as supports for nano-metal catalysts and there are a few examples of graphene-based solid acid catalyst (GSAC) (Narayanan et al., 2017). GSACs are mainly developed by sulfonic acid functionalization and successfully employed in several reactions including biomass conversion (Zhu et al., 2015), etherification of glycerol (Zhou et al., 2014), biodiesel production (Mahto et al., 2016), cyclization of hydrazides (Brahmayya et al., 2017), hydrolysis of ethyl acetate (Ji et al., 2011) and ester-exchange (Garg et al., 2014; Wang et al., 2013).

Phosphonic acid derivatives are superior to the sulfonated one in catalyzing specific reactions of hydrolysis, isomerization and dehydration mainly to the reduced tendency for reaction with organic materials (Dehn and Jackson, 1933). However, there are few reports on the phosphonated graphene substrates (Ghafuri and Talebi, 2016; Kim et al., 2016, 2014; Some et al., 2015) mainly due to the limited synthetic procedures associated with the phosphonic acid groups (Abouzari-lotf et al., 2011; Abouzari-Lotf et al., 2016) and difficult in controlling the functionalization level (Ghafuri and Talebi, 2016). Multi-step preparation procedure is used (Ghafuri and Talebi, 2016; Kim et al., 2016) and in some cases the functionalized catalyst becomes water soluble (Ghafuri and Talebi, 2016) which results in the inherent difficulty to recover the catalyst in the aqueous medium. Therefore, simple synthetic procedure with control over functionalization level is highly required to prepare proper phosphonated solid acid catalyst.

In this study, we prepared the phosphoric acid functionalized graphene oxide in a simple synthetic procedure capable of controlling the acid content. Following our recent efforts to use of heterogeneous catalysts in one-pot and multi-

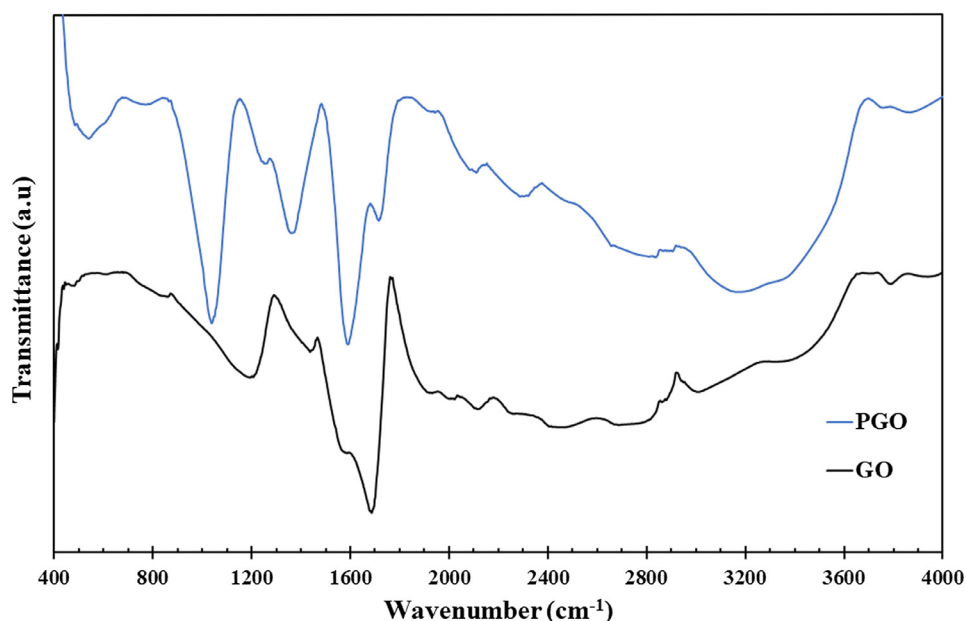


Fig. 3 FT-IR spectra of GO and phosphonated GO.

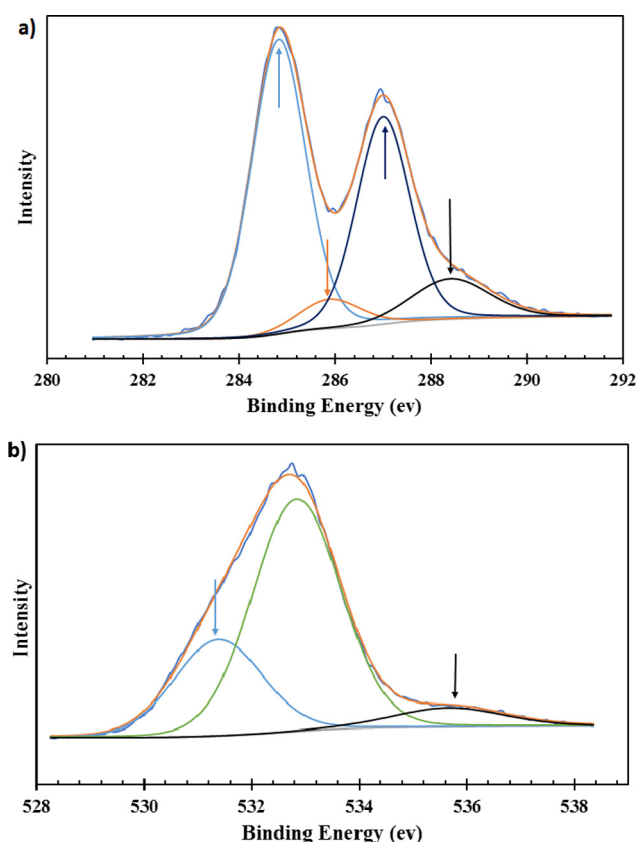


Fig. 4 High-resolution XPS spectra of phosphonated catalyst: (a) C 1s; (b) O 1s.

component reactions (Nasef et al., 2016; Zakeri et al., 2015a, 2015b, 2014), the catalytic performance of the developed nanocatalyst was evaluated in the similar reactions. The catalyst was used in the synthesis of biologically active

dihydropyrano[2,3-*c*]pyrazole derivatives in aqueous medium. To the best of our knowledge, this is the first example of using such functionalized solid acids in the multicomponent synthesis. The reaction is advantageous in terms of simple experimental and work-up procedure, excellent yields without need for column purification as well as short reaction time and eliminating the use of any toxic organic solvent.

## 2. Material and method

### 2.1. Materials

Graphite flakes (325 mesh), polyphosphoric acid (PPA, 105%  $\text{H}_3\text{PO}_4$  basis) and phosphoric acid (PA, analytical grade) were purchased from Sigma-Aldrich. All common reagents for the preparation of pyranopyrazoles were obtained from commercial suppliers and used without further purifications.

### 2.2. Characterizations

The chemical composition of the catalyst was characterized with Raman spectrometer (LabRAM HR Evo, Horiba), Fourier Transform Infrared attenuated total reflection spectroscopy (FTIR-ATR Thermo Fisher Scientific Nicolet iS50 spectrometer) and X-ray photoelectron spectroscopy (XPS, PHI Quantera II Scanning XPS Microprobe). The localized chemical composition (O/C and P/C ratios) and surface morphology were evaluated by Scanning Electron Microscope (SEM/EDX, Gemini SEM500). XRD diffraction pattern was obtained with the PANalytical Empyrean diffractometer with PIXcel<sup>3D</sup> detector over a range of  $2\theta = 4 - 70^\circ$ . The peak position was used to calculate interlayer spacing according to Bragg's equation ( $\lambda = 2d\sin\theta$ ).

The structure of the prepared pyrazoles was confirmed with  $^1\text{H}$  and  $^{13}\text{C}$  NMR spectroscopy at 400 and 100 MHz, respectively (BrukerAQS-AVANCE spectrometer using TMS as an

internal standard in DMSO-*d*<sub>6</sub> or CDCl<sub>3</sub>), FTIR-ATR and elemental analysis (Perkin Elmer 2004 (II) CHN analyzer). The melting points were measured using a capillary tube method with a Barnstead Electrothermal 9200 apparatus.

### 2.3. Preparation of phosphonated catalyst

The catalyst was prepared in a high yield procedure with three steps.

#### 2.3.1. Synthesis of GO

Oxidization of graphite flakes to graphite oxide and subsequent exfoliation were performed to achieve GO. Well-established modified Hummers and Offeman method was used to prepare graphite oxide (Kovtyukhova et al., 1999) Exfoliation to GO was achieved by ultrasonication of purified graphite oxide suspension using a Branson digital sonifier (SFX150, 150 w 40 kHz, 75% amplitude). Unexfoliated residual was removed by centrifugation at 4000 r.p.m in 10 °C for 15 min with a micro refrigerated centrifuge (model 3700, Kubota). The GO powder was obtained after drying in a vacuum oven at 70 °C for 24 h.

#### 2.3.2. Synthesis of phosphonated GO

The sonication was used to homogenize a 10 ml mixture of polyphosphoric acid and phosphoric acid (1/5, wt%/wt%). 0.4 M NaOH solution was added to adjust the pH of the solution to around 5. The solution was transferred into a 1 L 3-necked flask equipped with condenser, mechanical stirrer and thermometer. Finely dispersed GO in 50 mL deionized water (0.5 wt%) was added and the mixture was heated to 95 °C for 5, 10 and 15 h. The prepared samples are termed as GO-acid-I, GO-acid-II, and GO-acid-III, respectively. Finally, the highly-dispersed phosphonated GO was precipitated by ultra-high-speed centrifuge (at 11,000 rpm) at 2 °C and washed repeatedly with deionized water and dried under vacuum. The reaction was optimized by varying reaction time and comparing their C/P atomic ratios.

#### 2.4. General procedure for the synthesis of dihydropyrano[2,3-*c*] pyrazole derivatives

A mixture of aromatic aldehydes (2 mmol), malononitrile (0.13 g, 2 mmol), ethyl acetoacetate (0.26 g, 2 mmol), hydrazine hydrate (2.5 mmol) and phosphonated GO nanocatalyst

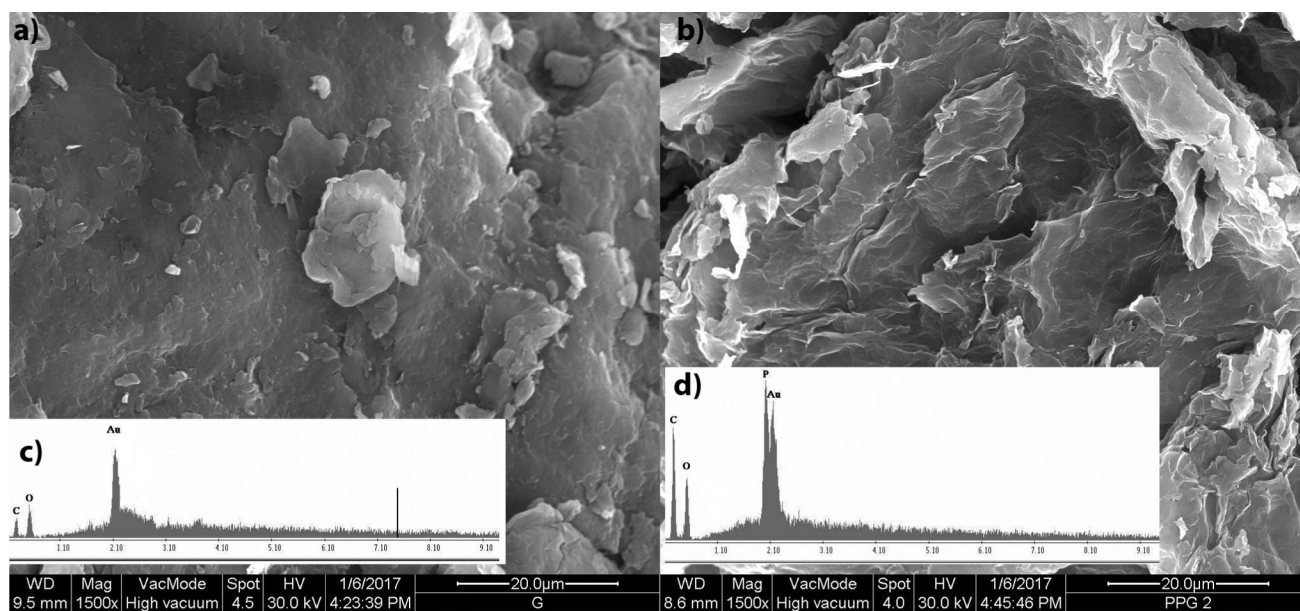


Fig. 5 SEM and EDX analysis of GO (a, c) and GO-PO<sub>3</sub>H<sub>2</sub> (b, d).

**Table 1** Elemental and functional characteristics of various acid functionalized nanocatalysts.

| Sample      | Composition <sup>a</sup> |       | I <sub>D</sub> /I <sub>G</sub> | Dispersibility in water  |
|-------------|--------------------------|-------|--------------------------------|--|
|             | O/C                      | P/C   |                                |  |
| GO          | 0.498                    | 0     | 0.815                          | Fine dispersed in water with short-term stability  |
| GO-acid-I   | 0.31                     | 0.07  | 0.952                          | Well dispersed in water and could be collected by centrifuging at low temperature                          |
| GO-acid-II  | 0.37                     | 0.115 | 0.960                          | Long-term stability of dispersed sample in water and could be collected by centrifuging at low temperature |
| GO-acid-III | 0.44                     | 0.125 | 0.984                          | Almost soluble in water and solution become clear  |

<sup>a</sup> Based on the EDX elemental analysis.



(5 mol% – of aldehydes) was refluxed at water media for an appropriate period of time. After completion of the reaction which was monitored by thin layer chromatography (TLC), the reaction mixture was cooled to room temperature and the precipitated organic product was decanted, washed with water ( $3 \times 10$  ml) and recrystallized from proper solvents to give the pure products. Then, the separation of the catalyst was carried out by centrifugation. The recycled catalyst was washed with ethanol (5 ml), dried in an oven under vacuum and used again for a sequential run under similar reaction conditions.

### 3. Result and discussion

#### 3.1. Synthesis and characterization of the nanocatalyst

Phosphonated GO was prepared from graphite in a three-step procedure of oxidation, exfoliation and phosphonation as shown in Fig. 1. The oxidation and exfoliation steps are well established methods to prepare graphene oxide (Hummers and Offeman, 1958; Kovtyukhova et al., 1999) Parameters of phosphonation step could be varied to achieve desired level of functionalization.

Successful exfoliation of Graphite was confirmed with XRD analysis as shown in the Fig. 2. The representative peaks of exfoliated GO and phosphonated GO was seen around  $2\theta = 9.7$ . The magnitude of XRD interlayer spacing shows that the distance among carbon layers have been increased slightly upon phosphonation and the value is around 1 nm. This enhancement can be due to the non-planar nature of phosphonic acid groups. The broad peak at  $2\theta$  around  $25^\circ$  of phosphonated graphene is due to the sample preparation as the nanocatalyst was deposited on a glass substrate.

Fig. 3 shows the changes in the IR spectrum upon phosphonation. As shown, the characteristic peaks for O–H stretching at  $3400\text{ cm}^{-1}$ , C=O stretching at around  $1690\text{ cm}^{-1}$ , C=C at  $1580\text{ cm}^{-1}$  and C–O stretching at  $1220\text{ cm}^{-1}$  have been seen for GO. Upon phosphonation, P–O, C<sub>ring</sub>–P and P=O peaks have been overlapped and seen as a broad peak centered at  $1040\text{ cm}^{-1}$ . Peak around  $1350\text{ cm}^{-1}$  may also be related to

phosphoric acid groups. In addition, C=O stretching peak was shifted to around  $1715\text{ cm}^{-1}$  upon phosphonation due to less involvement of carboxylic acids in the hydrogen bonding as the phosphonic acid groups are more involved in the stronger hydrogen bonds. Extended easily polarizable hydrogen bonding in phosphonated GO resulted in a broad band around  $2900\text{--}3600\text{ cm}^{-1}$ . Additionally, a weak-broad peak ending around  $620\text{ cm}^{-1}$  could be attributed to the P–C stretching.

As shown in Fig. S1, phosphonation reaction further confirmed by the XPS spectra as the P 2p and P 2s peaks were clearly found in the narrow scan at around 133.5 and 191.0 eV, respectively. To confirm the detailed structure, narrow scan of the C 1s and O 1s were deconvoluted as shown in the Fig. 4. C 1s revealed a peak at 284.4 eV which is attributed to the presence of C–C bond in the carbon structure of GO. The other peaks centered at 287 and 288.4 eV are assigned to C=O and C(O)OH. The small peak at 285.9 eV is assigned for C–P bond which indicates that the phosphonate groups have been attached to C atoms from the P sides. Deconvoluted O 1s revealed 3 peaks centered at 531.8, 532.8 and 535.8 eV corresponding to the C=O and P=O, C–O and P–O, and C(O)OH, respectively. It could be concluded that both forms of hydrolytically stable P–C bond and P–O–C of limited stability are formed during phosphonation.

EDX elemental analysis was used to calculate the phosphonation level. As shown in the Fig. 5 and summarized in the Table 1, the ratio of O/C has changed from 0.498 in GO to 0.31 in GO-acid-I and increased to 0.44 in GO-acid-III. On the other hand, the ratio of P/C has been increased from 0 in pristine graphene oxide to 0.125 in GO-acid-III. As shown in the SEM micrographs, as-prepared phosphonated catalyst and GO have almost the same graphene-like structures.

The calculated ration of I<sub>D</sub>/I<sub>G</sub> bands intensity in the Raman spectroscopy is another indication of the extent of defects on graphene materials. Fig. 6 shows the Raman spectra of the GO and GO-PO<sub>3</sub>H<sub>2</sub> with two clear broad peaks at  $1355$  and  $1580\text{ cm}^{-1}$  attributed to D and G bands, respectively. As seen, the intensity of D band (representing symmetry A<sub>1g</sub> mode typically results from the presence of sp<sup>3</sup> carbons or defects on

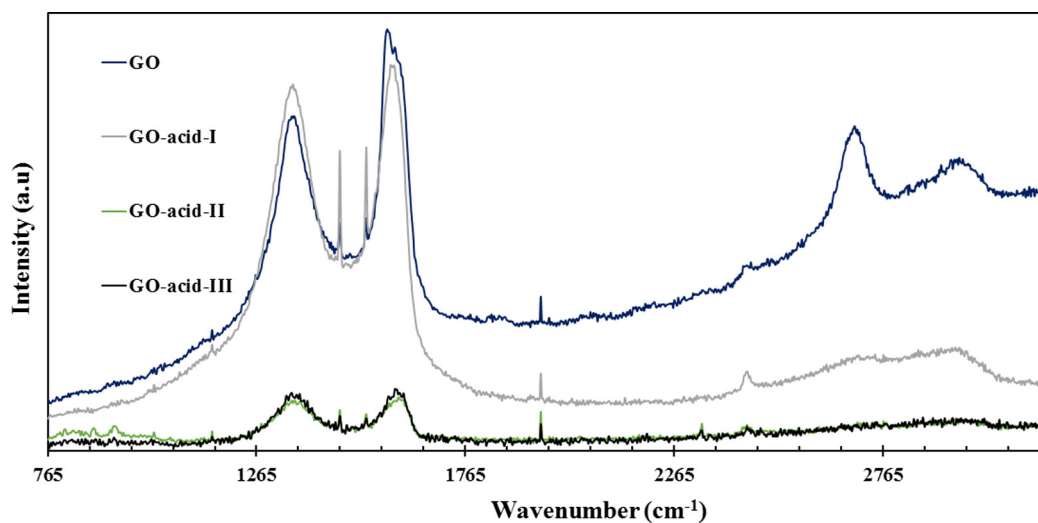


Fig. 6 Raman spectra of the GO and phosphonated GO.

the graphene sheets) is increasing in compared to G band (representing the  $E_{2g}$  mode of pristine  $sp^2$  carbon atoms). In addition, such broad D and G bands are clear indicative of a disordered chemical environment. An increment of the  $I_D/I_G$  ratio upon phosphonation from 0.815 to almost 1 (in Table 1) indicates the formation of large edges and defects on the phosphonated substrates. In addition, the other peaks assigned to 2D (two-phonon double resonance process) and S3 can be also seen at 2697 and 2947  $\text{cm}^{-1}$ . In the expanded 2D band area in Fig. S2, sharp band centered at 2697  $\text{cm}^{-1}$  was seen for GO with a full width half maximum (FWHM) of around 60  $\text{cm}^{-1}$ . This peak is indication of 2–3 layers GO. Upon phosphonation, the FWHM of the peak is clearly decreasing to around 40  $\text{cm}^{-1}$ . Such changes could be also considered as an indication of enhanced interlayer spacing.

### 3.2. Catalytic investigation of phosphonated GO nanocatalyst

The catalytic activity of the developed acid catalyst was evaluated in the synthesis of pyrano[2,3-*c*]pyrazoles. Such pyrazoles play an essential role as biologically active compounds and represent an interesting template in medicinal chemistry and pharmaceutical ingredients, such as anti-microbial, analgesic, anti-inflammatory, vasodilator and anti-fungicidal activities (Maity et al., 2017; Xie et al., 2016b) Varying grades of success have been reported for catalyzing the preparation of pyrano [2,3-*c*]pyrazoles using zirconium oxide, (Saha et al., 2015) ionic liquids, (Zakeri et al., 2017) silica-supported polyphosphoric

acid (Vekariya et al., 2016) and  $\text{NH}_4\text{H}_2\text{PO}_4/\text{Al}_2\text{O}_3$  (Maleki and Ashrafi, 2014) However, numerous limitations of low yields, use of expensive reagents, long reaction times, tedious work-up procedures with homogeneous catalyst, and co-occurrence of several side reactions have been reported. Consequently, the development of a general multicomponent reaction using an inexpensive, cleaner and green procedure leading to the pyrano[2,3-*c*]pyrazole derivatives is highly desirable.

Among the developed catalyst with various phosphonic acid content, GO-acid-II was selected for evaluation of the catalytic activity due to the easier recycling compared to GO-acid-III and more active sites compared to GO-acid-I. Fig. 7 represents the schematic of the multicomponent reaction assisted with GO-acid-II nanocatalyst.

The catalytic activity of the prepared nanocatalyst was evaluated in different conditions for the reaction of hydrazine hydrate, ethyl acetoacetate, benzaldehyde and malononitrile. As summarized in Table 2, several reactions were carried out to optimize the amount of required catalyst, best solvent and reaction time. The reaction under solvent-free condition at 80 and 120 °C afforded the products in low yields and reflux in water was drastically enhanced the yield. The screening of different solvents revealed that the phosphonated GO is more effective in polar-protic solvents such as ethanol and water compared to organic solvents (e.g.  $\text{CHCl}_3$ ,  $\text{CH}_2\text{Cl}_2$ , DMF, THF and  $\text{CH}_3\text{CN}$ ). The optimized conditions of 5 mol% catalyst, water as a reaction media and 15 min reaction time was achieved.

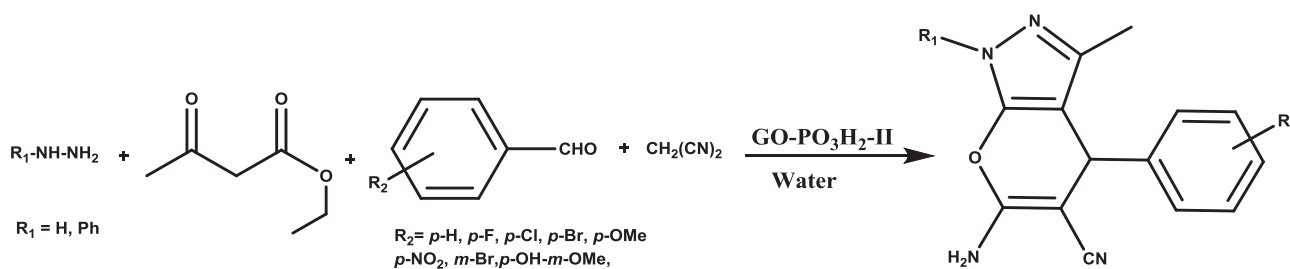


Fig. 7 The preparation of pyrano[2,3-*c*]pyrazoles using phosphonated GO as a nanocatalyst.

Table 2 Optimization of reaction parameters.

| Entry | Mol% of catalyst | Solvent                         | Temperature (°C) | Time (min) | Yield <sup>a</sup> (%) |
|-------|------------------|---------------------------------|------------------|------------|------------------------|
| 1     | 1                | H <sub>2</sub> O                | Reflux           | 30         | 45                     |
| 2     | 3                | H <sub>2</sub> O                | Reflux           | 30         | 65                     |
| 3     | 5                | H <sub>2</sub> O                | Reflux           | 15         | 90                     |
| 4     | 7                | H <sub>2</sub> O                | Reflux           | 15         | 90                     |
| 5     | 5                | EtOH                            | Reflux           | 30         | 75                     |
| 6     | 5                | CH <sub>3</sub> CN              | Reflux           | 30         | 55                     |
| 7     | 5                | CHCl <sub>3</sub>               | Reflux           | 30         | 50                     |
| 8     | 5                | CH <sub>2</sub> Cl <sub>2</sub> | Reflux           | 30         | 45                     |
| 9     | 5                | THF                             | Reflux           | 30         | Trace                  |
| 10    | 5                | DMF                             | Reflux           | 30         | Trace                  |
| 11    | 5                | – <sup>b</sup>                  | 80               | 30         | 60                     |
| 12    | 5                | – <sup>b</sup>                  | 120              | 30         | 75                     |

<sup>a</sup> Isolated yield.

<sup>b</sup> The mixture was stirred for 30 min then water was added and followed by stirring. Finally, the precipitated organic product was decanted, washed with water and recrystallized.

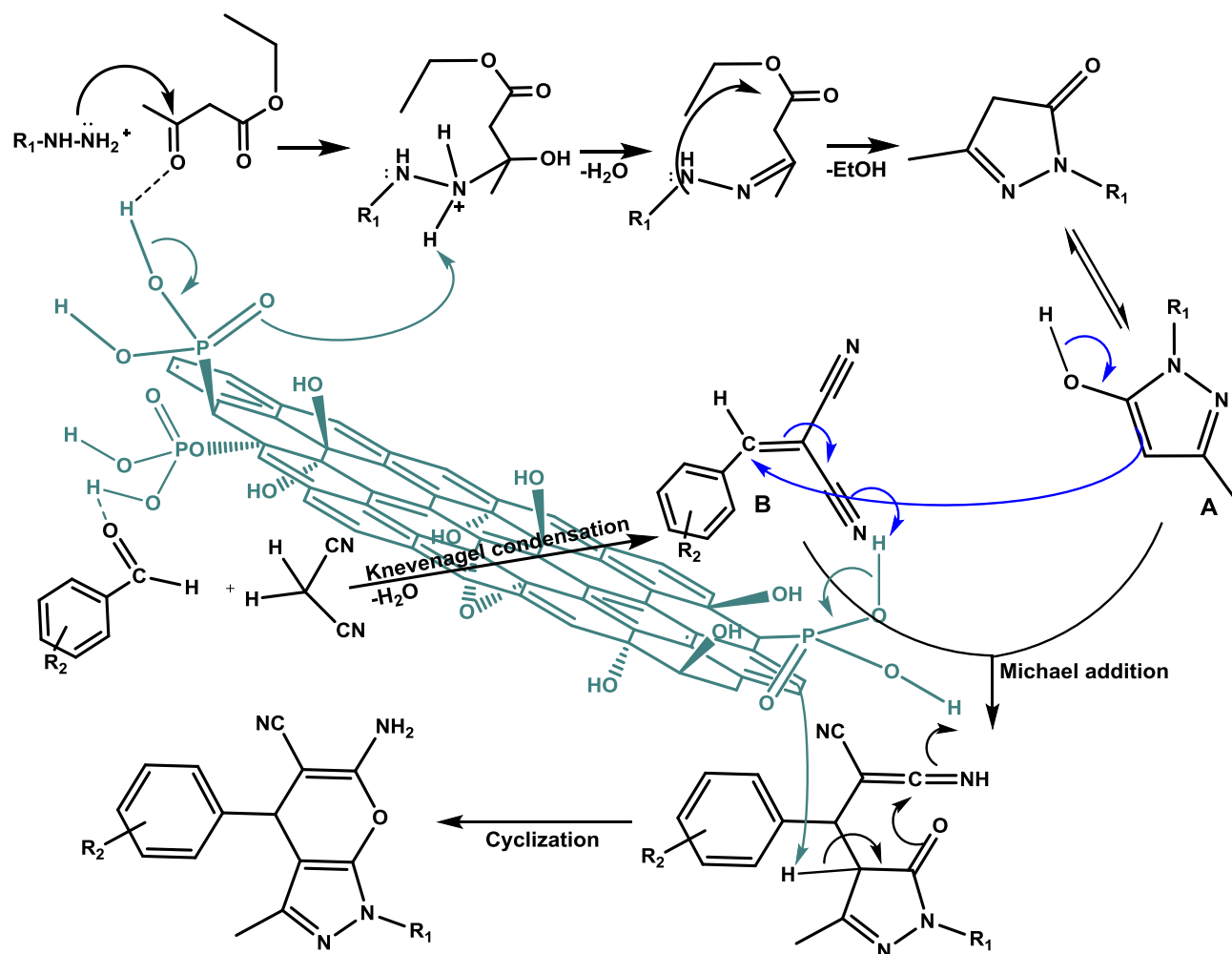


Fig. 8 Plausible mechanism for the formation of pyrano[2,3-*c*]pyrazole derivatives.

**Table 3** Reusability and recovery of the phosphonated GO nanocatalyst in water in the model reaction.

| Cycle | Recovered catalyst (%) | Reaction yield (%) |
|-------|------------------------|--------------------|
| 1     | 95                     | 90                 |
| 2     | 97                     | 90                 |
| 3     | 97                     | 89                 |
| 4     | 98                     | 88                 |
| 5     | 98                     | 90                 |
| 6     | 98                     | 89                 |

To explore the activity of the catalyst toward different substitutes, the generality of the multicomponent reaction was extended to a library of pyrano[2,3-*c*]pyrazole derivatives **5a-l** under the optimized reaction conditions. As summarized in [Table S1 in supporting information](#), a variety of aryl aldehydes (e.g.  $-\text{NO}_2$ ,  $-\text{CN}$ ,  $-\text{F}$ ,  $-\text{Cl}$ ,  $-\text{Br}$ ,  $-\text{OMe}$ ,  $-\text{OH}$ ) containing either electron withdrawing or electron donating groups afforded **5a-l** in good to excellent yields. The spectroscopy details of the prepared pyrazoles were summarized in the [supporting information](#). The high yield of 90% in short reaction time of 15 min was achieved due to presence of concerted func-

tional sites on the catalysts: both hydrophilic phosphoric acid and hydrophobic carbon sites together with acidic and basic sites of phosphate groups. As can be seen in [Table S1](#), the electronic effects of the substituent were not considerably altered the yields of the products. However, relatively low yields of the products were observed in case of phenyl hydrazine.

In a plausible mechanism, the formation of pyrano[2,3-*c*]pyrazole derivatives proceeds via the simultaneous formation of two intermediates, pyrazolone **A** via cyclo condensation and arylidene malononitrile **B** by Knoevenagel condensation reaction as shown in [Fig. 8](#). Intermediate **A** was formed by the attack of phenylhydrazine to carbonyl group of the activated ethyl acetoacetate followed with the loss of water and continued with intramolecular nucleophilic attack by another amine group of phenylhydrazine to the next carbonyl group of ethyl acetoacetate. In the next step, formation of the intermediate **B** was occurred via Knoevenagel condensation between malononitrile and activated benzaldehyde, followed by loss of water molecules. Subsequently, intermediate **A** undergoes Michael addition with **B** in the presence of catalyst. The reaction was followed by intramolecular nucleophilic attack and cyclization to afford the expected dihydropyrano [2,3-*c*]pyrazole derivative. As shown, the amphoteric nature

of the phosphonic acid is playing a role in the proposed mechanism and both of.

### 3.3. Reusability study of the phosphonated catalyst

The recovery and reusability are among the most important criteria in developing alternative catalysts. Even though the catalyst dispersion is one of the important advantages of phosphonated materials, it can negatively affect the catalyst recovery. In the synthesis of pyrazoles, the catalyst was collected after each reaction by centrifuging at low temperature and amount of retrieved catalyst was taken as an indication of the recovery. The recovered catalyst was tested for the similar reaction under the identical conditions and the reaction yield was considered as an indication of catalyst stability. As summarized in the Table 3, the catalyst can be reused at least six times with retention of its catalytic performance. However, a slight decrease in recovery was observed mainly after the first run. It could be due to the solubility of highly functionalized and/or small sized nanocatalysts.

## 4. Conclusion

A new type of highly dispersible phosphoric acid functionalized carbon based nanocatalysts was prepared in a simple synthetic procedure. The catalytic activity of developed catalyst was evaluated toward the synthesis of pyrano[2,3-*c*]pyrazoles in one-pot, four-component reaction of hydrazines, malononitrile, ethyl acetoacetate and aldehydes in water. The reaction afforded pyrazoles with excellent yield of 80–90% which is an indication of high catalyst activity. Moreover, it was found that the catalyst is highly stable, could be recovered easily and the catalyst activity remained almost unchanged after 6 catalytic cycles. The newly prepared phosphoric acid functionalized graphene oxide catalyst has multi-functions with both hydrophilic acid and hydrophobic carbon sheet sites as well as functional groups with acidic and basic sites. Such multi-functional catalysts can be applicable for large-scale green synthesis of wide variety of chemical reactions of multi-components with different characteristics.

## Acknowledgment

The research was primarily supported by Ministry of Higher Education under Fundamental Research Grant (vote no. #4F775) as well as Research University Fund Scheme of Universiti Teknologi Malaysia (vote no. #17H21). M. Zakeri is thankful for the financial support from Malaysia–Japan International Institute of Technology (vote no. #00580).

## Appendix A. Supplementary material

Supplementary data associated with this article can be found, in the online version, at <https://doi.org/10.1016/j.arabjc.2017.11.006>.

## References

Abouzari-Lotf, E., Ghassemi, H., Mehdipour-Ataei, S., Shockravi, A., 2016. Phosphonated polyimides: enhancement of proton conduc-

- tivity at high temperatures and low humidity. *J. Memb. Sci.* 516, 74–82. <https://doi.org/10.1016/j.memsci.2016.06.009>.
- Abouzari-lotf, E., Ghassemi, H., Shockravi, A., Zawodzinski, T., 2011. Phosphonated poly (arylene ether) s as potential high temperature proton conducting materials. *Polymer (Guildf)* 52, 4709–4717. <https://doi.org/10.1016/j.polymer.2011.08.020>.
- Al-Marri, A.H., Khan, M., Shaik, M.R., Mohri, N., Adil, S.F., Kuniyil, M., Alkathlan, H.Z., Al-Warthan, A., Tremel, W., Tahir, M.N., Khan, M., Siddiqui, M.R.H., 2016. Green synthesis of Pd@graphene nanocomposite: catalyst for the selective oxidation of alcohols. *Arab. J. Chem.* 9, 835–845. <https://doi.org/10.1016/j.arabjc.2015.12.007>.
- Ameta, C., Ameta, K.L., 2014. Water: a benign solvent for the synthesis of various organic moieties. In: Ameta, K.L., Dandia, A. (Eds.), *Green Chemistry: Synthesis of Bioactive Heterocycles*. Springer, India, New Delhi, pp. 231–252. [https://doi.org/10.1007/978-81-322-1850-0\\_8](https://doi.org/10.1007/978-81-322-1850-0_8).
- Antonyraj, C.A., Kim, B., Kim, Y., Shin, S., Lee, K.-Y., Kim, I., Cho, J.K., 2014. Heterogeneous selective oxidation of 5-hydroxymethyl-2-furfural (HMF) into 2,5-diformylfuran catalyzed by vanadium supported activated carbon in MIBK, extracting solvent for HMF. *Catal. Commun.* 57, 64–68. <https://doi.org/10.1016/j.catecom.2014.08.008>.
- Brahmayya, M., Dai, S.A., Suen, S.-Y., 2017. Sulfonated reduced graphene oxide catalyzed cyclization of hydrazides and carbon dioxide to 1,3,4-oxadiazoles under sonication. *Sci. Rep.* 7, 4675. <https://doi.org/10.1038/s41598-017-04143-4>.
- Chanda, A., Fokin, V.V., 2009. Organic synthesis “on water”. *Chem. Rev.* 109, 725–748. <https://doi.org/10.1021/cr800448q>.
- Chen, L., Nohair, B., Kaliaguine, S., 2016. Glycerol acetalization with formaldehyde using water-tolerant solid acids. *Appl. Catal. A Gen.* 509, 143–152. <https://doi.org/10.1016/j.apcata.2015.08.014>.
- Chen, M., Liang, C., Zhang, F., Li, H., 2014. ACS Sustain. Chem. Eng. 2, 486–492. <https://doi.org/10.1021/sc400391r>.
- Chinthaginjala, J.K., Seshan, K., Lefferts, L., 2007. Preparation and application of carbon-nanofiber based microstructured materials as catalyst supports. *Ind. Eng. Chem. Res.* 46, 3968–3978. <https://doi.org/10.1021/ie061394r>.
- Cole, A.C., Jensen, J.L., Ntai, I., Tran, K.L.T., Weaver, K.J., Forbes, D.C., Davis, J.H., 2002. Novel Brønsted acidic ionic liquids and their use as dual solvent–catalysts. *J. Am. Chem. Soc.* 124, 5962–5963. <https://doi.org/10.1021/ja026290w>.
- Dehn, W.M., Jackson, K.E., 1933. Phosphoric acid in organic reactions. *J. Am. Chem. Soc.* 55, 4284–4287. <https://doi.org/10.1021/ja01337a070>.
- Garg, B., Bisht, T., Ling, Y.-C., 2014. Sulfonated graphene as highly efficient and reusable acid carbocatalyst for the synthesis of ester plasticizers. *RSC Adv.* 4, 57297–57307. <https://doi.org/10.1039/C4RA11205A>.
- Georgakilas, V., Tiwari, J.N., Kemp, K.C., Perman, J.A., Bourlinos, A.B., Kim, K.S., Zboril, R., 2016. Noncovalent functionalization of graphene and graphene oxide for energy materials, biosensing, catalytic, and biomedical applications. *Chem. Rev.* 116, 5464–5519. <https://doi.org/10.1021/acs.chemrev.5b00620>.
- Ghafuri, H., Talebi, M., 2016. Water-soluble phosphated graphene: preparation, characterization, catalytic reactivity, and adsorption property. *Ind. Eng. Chem. Res.* 55, 2970–2982. <https://doi.org/10.1021/acs.iecr.5b02250>.
- Gromov, N.V., Taran, O.P., Semeykina, V.S., Danilova, I.G., Pestunov, A.V., Parkhomchuk, E.V., Parmon, V.N., 2017. Solid acidic NbO<sub>x</sub>/ZrO<sub>2</sub> catalysts for transformation of cellulose to glucose and 5-hydroxymethylfurfural in pure hot water. *Catal. Lett.* 147, 1485–1495. <https://doi.org/10.1007/s10562-017-2056-y>.
- Gupta, P., Paul, S., 2014. Solid acids: green alternatives for acid catalysis. *Catal. Today* 236, 153–170. <https://doi.org/10.1016/j.cattod.2014.04.010>.
- Hajipour, A.R., Khorsandi, Z., 2016. Multi walled carbon nanotubes supported N-heterocyclic carbene–cobalt (II) as a novel, efficient



- and inexpensive catalyst for the Mizoroki-Heck reaction. *Catal. Commun.* 77, 1–4. <https://doi.org/10.1016/j.catcom.2015.12.027>.
- Hummers, W.S., Offeman, R.E., 1958. Preparation of graphitic oxide. *J. Am. Chem. Soc.* 80. <https://doi.org/10.1021/ja01539a017>. 1339–1339.
- Jamil, F., Al-Muhtaseb, A.H., Naushad, M., Baawain, M., Al-Mamun, A., Saxena, S.K., Viswanadham, N., 2017. Evaluation of synthesized green carbon catalyst from waste date pits for tertiary butylation of phenol. *J. Chem. Arab.* <https://doi.org/10.1016/j.arabjc.2017.04.009>.
- Ji, J., Zhang, G., Chen, H., Wang, S., Zhang, G., Zhang, F., Fan, X., 2011. Sulfonated graphene as water-tolerant solid acid catalyst. *Chem. Sci.* 2, 484–487. <https://doi.org/10.1039/C0SC00484G>.
- Karimi, B., Zareyee, D., 2008. Design of a highly efficient and water-tolerant sulfonic acid nanoreactor based on tunable ordered porous silica for the von Pechmann reaction. *Org. Lett.* 10, 3989–3992. <https://doi.org/10.1021/ol8013107>.
- Kim, K.J., Lee, H.S., Kim, J., Park, M.-S., Kim, J.H., Kim, Y.-J., Skyllas-Kazacos, M., 2016. Superior electrocatalytic activity of a robust carbon-felt electrode with oxygen-rich phosphate groups for all-vanadium redox flow batteries. *ChemSusChem* 9, 1329–1338. <https://doi.org/10.1002/cssc.201600106>.
- Kim, M.-J., Jeon, I.-Y., Seo, J.-M., Dai, L., Baek, J.-B., 2014. Graphene phosphonic acid as an efficient flame retardant. *ACS Nano* 8, 2820–2825. <https://doi.org/10.1021/nl4066395>.
- Kovtyukhova, N.I., Ollivier, P.J., Martin, B.R., Mallouk, T.E., Chizhik, S.A., Buzaneva, E.V., Gorchinskiy, A.D., 1999. Layer-by-layer assembly of ultrathin composite films from micron-sized graphite oxide sheets and polycations. *Chem. Mater.* 11, 771–778. <https://doi.org/10.1021/cm981085u>.
- Li, F., Kang, W., Cheng, B., Dong, Y., 2015. Preparation and catalytic behavior of hollow Ag/carbon nanofibers. *Catal. Commun.* 69, 150–153. <https://doi.org/10.1016/j.catcom.2015.05.030>.
- Lin, X.-Z., Ren, T.-Z., Yuan, Z.-Y., 2015. Mesoporous zirconium phosphonate materials as efficient water-tolerable solid acid catalysts. *Catal. Sci. Technol.* 5, 1485–1494. <https://doi.org/10.1039/C4CY01110D>.
- Liu, P., Wang, H., Yan, T., Zhang, J., Shi, L., Zhang, D., 2016. Grafting sulfonic and amine functional groups on 3D graphene for improved capacitive deionization. *J. Mater. Chem. A* 4, 5303–5313. <https://doi.org/10.1039/C5TA10680J>.
- Liu, Y., Mo, K., Cui, Y., 2013. Porous and robust lanthanide metal-organoboron frameworks as water tolerant lewis acid catalysts. *Inorg. Chem.* 52, 10286–10291. <https://doi.org/10.1021/ic400598x>.
- Lv, M., Xie, W., Sun, S., Wu, G., Zheng, L., Chu, S., Gao, C., Bao, J., 2015. Activated-carbon-supported K-Co-Mo catalysts for synthesis of higher alcohols from syngas. *Catal. Sci. Technol.* 5, 2925–2934. <https://doi.org/10.1039/C5CY00083A>.
- Mahto, T.K., Jain, R., Chandra, S., Roy, D., Mahto, V., Sahu, S.K., 2016. Single step synthesis of sulfonic group bearing graphene oxide: a promising carbo-nano material for biodiesel production. *J. Environ. Chem. Eng.* 4, 2933–2940. <https://doi.org/10.1016/j.jece.2016.06.006>.
- Maity, R., Gharui, C., Sil, A.K., Pan, S.C., 2017. Organocatalytic asymmetric michael/hemiketalization/retro-aldol reaction of  $\alpha$ -nitroketones with unsaturated pyrazolones: synthesis of 3-acyloxy pyrazoles. *Org. Lett.* 19, 662–665. <https://doi.org/10.1021/acs.orglett.6b03823>.
- Maleki, B., Ashrafi, S.S., 2014. Nano  $\alpha$ -Al<sub>2</sub>O<sub>3</sub> supported ammonium dihydrogen phosphate (NH<sub>4</sub>H<sub>2</sub>PO<sub>4</sub>/Al<sub>2</sub>O<sub>3</sub>): preparation, characterization and its application as a novel and heterogeneous catalyst for the one-pot synthesis of tetrahydrobenzo[b]pyran and pyrano [2,3-*c*]pyrazole deri. *RSC Adv.* 4, 42873–42891. <https://doi.org/10.1039/C4RA07813F>.
- Narayanan, D.P., Gopalakrishnan, A., Yaakob, Z., Sugunan, S., Narayanan, B.N., 2017. A facile synthesis of clay – graphene oxide nanocomposite catalysts for solvent free multicomponent Biginelli reaction. *J. Chem. Arab.* <https://doi.org/10.1016/j.arabjc.2017.04.011>.
- Nasef, M.M., Zakeri, M., Asadi, J., Abouzari-Lotf, E., Ahmad, A., Malakooti, R., 2016. Environmentally benign and highly regioselective ring opening of epoxides accelerated by ultrasound irradiation. *Green Chem. Lett. Rev.* 9. <https://doi.org/10.1080/17518253.2015.1137975>.
- Navalon, S., Dhakshinamoorthy, A., Alvaro, M., Garcia, H., 2014. Carbocatalysis by graphene-based materials. *Chem. Rev.* 114, 6179–6212. <https://doi.org/10.1021/cr4007347>.
- Okuhara, T., 2002. Water-tolerant solid acid catalysts. *Chem. Rev.* 102, 3641–3666. <https://doi.org/10.1021/cr0103569>.
- Saha, A., Payra, S., Banerjee, S., 2015. One-pot multicomponent synthesis of highly functionalized bio-active pyrano[2,3-*c*]pyrazole and benzylpyrazolyl coumarin derivatives using ZrO<sub>2</sub> nanoparticles as a reusable catalyst. *Green Chem.* 17, 2859–2866. <https://doi.org/10.1039/C4GC02420F>.
- Sangshetti, J.N., Dharmadhikari, P.P., Chouthe, R.S., Fatema, B., 2017. Water mediated oxalic acid catalyzed one pot synthesis of 1,8-dioxodecahydroacridines. *Arab. J. Chem.* 10, S10–S12. <https://doi.org/10.1016/j.arabjc.2012.06.005>.
- Sengupta, A., Su, C., Bao, C., Nai, C.T., Loh, K.P., 2014. Graphene oxide and its functionalized derivatives as carbocatalysts in the multicomponent strecker reaction of ketones. *ChemCatChem* 6, 2507–2511. <https://doi.org/10.1002/cctc.201402254>.
- Shen, F., Smith, R.L., Li, L., Yan, L., Qi, X., 2017. Eco-friendly method for efficient conversion of cellulose into levulinic acid in pure water with cellulase-mimetic solid acid catalyst. *ACS Sustain. Chem. Eng.* 5, 2421–2427. <https://doi.org/10.1021/acssuschemeng.6b02765>.
- Simon, M.-O., Li, C.-J., 2012a. Green chemistry oriented organic synthesis in water. *Chem. Soc. Rev.* 41, 1415–1427. <https://doi.org/10.1039/C1CS15222J>.
- Simon, M.-O., Li, C.-J., 2012b. Organic synthesis in water. In: *Green Techniques for Organic Synthesis and Medicinal Chemistry*. John Wiley & Sons, Ltd, Chichester, UK, pp. 263–295. <https://doi.org/10.1002/9780470711828.ch10>.
- Some, S., Shackery, I., Kim, S.J., Jun, S.C., 2015. Phosphorus-doped graphene oxide layer as a highly efficient flame retardant. *Chem. – Eur. J.* 21, 15480–15485. <https://doi.org/10.1002/chem.201502170>.
- Su, D.S., Perathoner, S., Centi, G., 2013. Nanocarbons for the development of advanced catalysts. *Chem. Rev.* 113, 5782–5816. <https://doi.org/10.1021/cr300367d>.
- Sun, X., Wang, W., Wu, T., Qiu, H., Wang, X., Gao, J., 2013. Grafting of graphene oxide with poly(sodium 4-styrenesulfonate) by atom transfer radical polymerization. *Mater. Chem. Phys.* 138, 434–439. <https://doi.org/10.1016/j.matchemphys.2012.12.022>.
- Tang, P., Hu, G., Li, M., Ma, D., 2016. Graphene-based metal-free catalysts for catalytic reactions in the liquid phase. *ACS Catal.* 6, 6948–6958. <https://doi.org/10.1021/acscatal.6b01668>.
- Vekariya, R.H., Prajapati, N.P., Patel, H.D., 2016. Silica-supported polyphosphoric acid (PPA-SiO<sub>2</sub>): an efficient and reusable heterogeneous catalyst for ecofriendly organic synthesis. *Synth. Commun.* 46, 197–219. <https://doi.org/10.1080/00397911.2015.1114633>.
- Wang, L., Wang, D., Zhang, S., Tian, H., 2013. Synthesis and characterization of sulfonated graphene as a highly active solid acid catalyst for the ester-exchange reaction. *Catal. Sci. Technol.* 3, 1194. <https://doi.org/10.1039/c3cy20646g>.
- Xie, J., Torres Galvis, H.M., Koeken, A.C.J., Kirilin, A., Dugulan, A. I., Ruitenbeek, M., de Jong, K.P., 2016a. Size and promoter effects on stability of carbon-nanofiber-supported iron-based Fischer-Tropsch catalysts. *ACS Catal.* 6, 4017–4024. <https://doi.org/10.1021/acscatal.6b00321>.
- Xie, J., Xing, X.-Y., Sha, F., Wu, Z.-Y., Wu, X.-Y., 2016b. Enantioselective synthesis of spiro[indoline-3,4'-pyrano[2,3-*c*]pyrazole] derivatives via an organocatalytic asymmetric Michael/cyclization cascade reaction. *Org. Biomol. Chem.* 14, 8346–8355. <https://doi.org/10.1039/C6OB01256F>.

- Zakeri, M., Nasef, M.M., Abouzari-Lotf, E., 2014. Eco-safe and expeditious approaches for synthesis of quinazoline and pyrimidine-2-amine derivatives using ionic liquids aided with ultrasound or microwave irradiation. *J. Mol. Liq.* 199. <https://doi.org/10.1016/j.molliq.2014.09.018>.
- Zakeri, M., Nasef, M.M., Abouzari-Lotf, E., Haghi, H., 2015a. Ultrasound-assisted regioselective ring opening of epoxides with nitrogen heterocycles using pyrrolidonium and imidazolium-based acidic ionic liquids. *Res. Chem. Intermed.* 41. <https://doi.org/10.1007/s11164-015-2015-4>.
- Zakeri, M., Nasef, M.M., Abouzari-Lotf, E., Moharami, A., Heravi, M.M., 2015b. Sustainable alternative protocols for the multicomponent synthesis of spiro-4H-pyrans catalyzed by 4-dimethylaminopyridine. *J. Ind. Eng. Chem.* 29, 273–281. <https://doi.org/10.1016/j.jiec.2015.03.035>.
- Zakeri, M., Nasef, M.M., Kargaran, T., Ahmad, A., Abouzari-Lotf, E., Asadi, J., 2017. Synthesis of pyrano[2,3-*c*]pyrazoles by ionic liquids under green and eco-safe conditions. *Res. Chem. Intermed.* 43. <https://doi.org/10.1007/s11164-016-2648-y>.
- Zhou, J., Wang, Y., Guo, X., Mao, J., Zhang, S., 2014. Etherification of glycerol with isobutene on sulfonated graphene: reaction and separation. *Green Chem.* 16, 4669–4679. <https://doi.org/10.1039/C4GC01044B>.
- Zhu, S., Wang, J., Fan, W., 2015. Graphene-based catalysis for biomass conversion. *Catal. Sci. Technol.* 5, 3845–3858. <https://doi.org/10.1039/C5CY00339C>.